Oxidized low-density lipoprotein-induced p62/SQSTM1 accumulation in THP-1-derived macrophages promotes IL-18 secretion and cell death

HAOFENG NING, DAN LIU, XIAOCHEN YU and XIURU GUAN

Department of Laboratory Diagnostics, The First Affiliated Hospital of Harbin Medical University, Harbin, Heilongjiang 150001, P.R. China

Received July 27, 2016; Accepted October 5, 2016

DOI: 10.3892/etm.2017.5221

Abstract. Macrophage autophagy has a protective role in the development of atherosclerosis; however, it turns dysfunctional in advanced lesions with an increase in p62/sequestosome-1 protein. Little is known about the role and significance of p62 accumulation in atherosclerosis. The present study investigated the association between p62 expression and the process of foam cell formation. Foam cell models were established through incubation of THP-1-derived macrophages with oxidized low-density lipoprotein, and the process of foam cell formation was detected by Oil red O staining. Furthermore, the dynamic change of p62 expression was detected by western blotting and quantitative polymerase chain reaction. Additionally, using gene silencing techniques, the roles of p62 in foam cells were investigated with ELISA, MTT and flow cytometry. The results indicated that besides serving as a marker of autophagy deficiency, the p62 protein could also mediate inflammation and cytotoxicity in advanced foam cells. Additionally, the implication of p62 in autophagy inhibition and foam cell formation makes it a key atherogenic factor under autophagy-deficient conditions.

Introduction

Annually, cardiovascular disease (CVD) is responsible for >17 million mortalities around the world, and is known as a disorder with the largest mortality rates globally (1). Atherosclerosis, which is characterized by lipid accumulation and long-term inflammation within the arteries, composes the major underlying pathology of CVD (2). It is generally considered that unstable atherosclerotic plaques are responsible for acute cardiovascular complications, including myocardial infarction, stroke and sudden cardiac death (3).

Of several cells associated with plaque stability, macrophages that are derived from the differentiation of monocyte precursors upon migration into the sub-endothelial space (4,5) are critical in progressive plaque formation. By the large uptake of accumulated lipids, particularly the modified low-density lipoprotein (LDL), macrophages turn into lipid-filled foam cells, leading to the secretion of pro-inflammatory cytokines and the establishment of a positive feedback loop for further monocyte recruitment and intima migration (6,7).

Macrophage macroautophagy (hereafter referred to as autophagy), which may affect apoptosis and efferocytosis, links lipid metabolism and the inflammatory response to the development of atherosclerotic lesions (8,9). In the lipid-excessive environment of plaques, the autophagy-lysosomal system degrades cytoplasmic lipid droplets and damaged organelles, as well as misfolded proteins within macrophages, indicating that autophagy has a pivotal protective role in preventing the composition and progression of foam cells (10). However, autophagy becomes dysfunctional as lesion development progresses (11,12). Notably, accompanying the deficient autophagy, an evident increase in the p62/sequestosome-1 (SQSTM1) protein level (hereafter referred to as p62) appears in macrophage-rich areas of atherosclerotic aortas (8,9).

p62, an autophagy receptor molecule and a selective autophagic substrate, may associate with ubiquitin-tagged proteins and organelles and deliver them to the lysosome for degradation (13). p62 is also a scaffold protein with several domains that is implicated in various signal transduction pathways, including nuclear factor (NF)-κB, NF erythroid 2-related factor 2, mitogen-activated protein kinase and mechanistic target of rapamycin (mTOR) (14,15). Increasing reports have indicated that p62 has multiple pathophysiological functions in the inflammatory response, metabolism regulation, inclusion body formation and tumorigenesis (16,17). However, the regulation and significance of p62 during atherosclerosis development have not been characterized.

As an independent risk factor of atherosclerosis, oxidized LDL (oxLDL) exhibits a variety of atherogenic properties, including promoting foam cell formation and the inflammatory response (10,18). In order to investigate the correlation

Correspondence to: Dr Xiuru Guan, Department of Laboratory Diagnostics, The First Affiliated Hospital of Harbin Medical University, 199 Dongdazhi, Harbin, Heilongjiang 150001, P.R. China
E-mail: gxr0451@sina.com

Key words: p62/sequestosome-1, autophagy, macrophages, oxidized low-density lipoprotein, atherosclerosis

between p62 expression and oxLDL-induced foam cell formation, the present study utilized THP-1-derived macrophages (THP-M) as a cell model.

Materials and methods

Antibodies and reagents. The following primary antibodies were obtained for the present study: p62/SQSTM1 (cat. no. 8025S; Cell Signaling Technology, Inc., Danvers, MA, USA); light-chain 3 (LC3)B (cat. no. L7543); and β-actin (cat. no. A1987) (Sigma-Aldrich; Merck KGaA, Darmstadt, Germany). Horseradish peroxidase-conjugated secondary antibodies were purchased from OriGene Technologies, Inc., (cat. nos. TA-130003 and TA140003, respectively; Rockville, MD, USA) and chloroquine (CQ) diphosphate salt was purchased from Sigma-Aldrich (cat. no. C6628; Merck KGaA).

Cell culture. Human monocyte cell line, THP-1, was purchased from the Type Culture Collection of the Chinese Academy of Sciences (Shanghai, China). Cells were maintained in RPMI-1640 medium supplemented with 2 mM L-glutamine and 100 U/ml streptomycin-penicillin (Hyclone; GE Healthcare Life Sciences, Logan, UT, USA), and 10% heat-inactivated fetal bovine serum (Gibco; Thermo Fisher Scientific, Inc., Waltham, MA, USA) at 37˚C with 5% CO_2. THP-1 cells were plated in 6-well culture plates at $1x10^6$ cells/well and were differentiated to macrophages using 100 ng/ml phorbol-12-myristate-13-acetate (PMA; Sigma-Aldrich; Merck KGaA) for 24 h with serum-free RPMI-1640 at 37˚C. Additionally, oxLDL (Guangzhou Yiyuan Biological Technology Co., Ltd., Guangzhou, China) was added to a final concentration of 20 μg/ml to induce foam cell formation.

Small interfering RNA (siRNA) knockdown of p62/SQSTM1. p62/SQSTM1 siRNA (sc-29679) and control (con) siRNA (sc-37007) were purchased from Santa Cruz Biotechnology, Inc., (Dallas, TX, USA) (sequences were not released by the company). For differentiation of THP-1 cells, 100 ng/ml PMA was used. Following differentiation, a total of $2x10^5$ cells/well were grown in 6-well plates with 2 ml serum-free RPMI-1640, and transfected with 50 nM of each siRNA for 48 h using a HiPerfect Transfection reagent (Qiagen, Inc., Valencia, CA, USA) at 37˚C. The SQSTM1 mRNA levels were examined by reverse transcription-quantitative polymerase chain reaction (RT-qPCR), and western blotting was utilized to verify the efficacy of protein knockdown by siRNA.

Oil Red O staining. Following incubation with oxLDL, THP-M cells were fixed with 4% formalin for 10 min at room temperature, and then stained with Oil Red O solution (0.5% Oil Red O in 60% isopropanol) for 15 min at 37˚C. Foam cell formation was observed under an inverted light microscope (magnification, x100 and x40), and the accumulated lipid droplets in the cells were stained red. Furthermore, the uptake of oxLDL was examined by extracting the intracellular Oil Red O in isopropanol and by measuring the optical density (OD) at 520 nm. Another replicate experiment was performed at the same time for correcting the cell number and size in different samples. Finally, the degree of lipid droplets was quantified on the basis of the mean OD value for average cells, which converts an OD value of ~$1x10^6$ cells/ml isopropanol (19,20).

Western blotting. Cells were lysed in ice-cold RIPA lysis buffer (POO13C; Beyotime, Shanghai, China). The protein concentration was determined by BCA method. The total protein samples (40 μg) were separated on 12% SDS-PAGE gels and transferred onto polyvinylidene difluoride membranes (EMD Millipore, Billerica, MA, USA). Following blocking with Tris-buffered saline and Tween-20 containing 5% non-fat dry skimmed-milk for 1 h at room temperature, membranes were incubated overnight with the previously mentioned primary antibodies (p62/SQSTM1, 1:1,000 dilution; LC3B, 1:1,000 dilution; and β-actin, 1:1,000 dilution) at 4˚C. The appropriate horseradish peroxidase-conjugated secondary antibodies (goat anti-mouse IgG, 1:5,000 dilution; goat anti-rabbbit IgG, 1:5,000 dilution) were applied for 1 h at room temperature, and immunoreactivity was subsequently visualized using a WesternBright enhanced chemiluminescent kit (Advansta, Inc., Menlo Park, CA, USA). Furthermore, densitometric analyses were performed using an imaging analyzer (Tanon 5200; Tanon Science and Technology Co., Ltd., Shanghai, China) and Tanon Gis software (Gel Image System Ver. 4.00; Tanon Science and Technology Co., Ltd.). Experiments were performed in triplicate.

Based on the method described above, firstly, the conversion of LC3-I to LC3-II was determined by western blotting in order to evaluate the activity of autophagic initiation. Subsequently, the activity of autophagic flux was assessed by using chloroquine (CQ), a specific lysosomal inhibitor that interferes with vesicular acidification. A total of $2x10^5$ cells/well were grown in 6-well plates with 2 ml serum-free RPMI-1640 and transfected with 50 nM con siRNA or p62 siRNA for 48 h using a HiPerfect Transfection reagent. Western blotting was subsequently performed with the anti-LC3B antibody following exposure to 20 μg/ml oxLDL for the indicated time, with or without CQ (30 μM) for the last 2 h.

RT-qPCR. Total cellular RNA was isolated using TRIzol reagent (Invitrogen; Thermo Fisher Scientific, Inc.), according to the manufacturer's instructions, and the integrity was confirmed by electrophoresis on an ethidium bromide-stained 1.5% agarose gel. cDNA was generated with an AccuPower RT PreMix (Bioneer Corp., Daejeon, Korea), according to the manufacturer's instructions. qPCR was then performed using an AccuPower GreenStar qPCR PreMix (Bioneer Corp.), according to the manufacturer's instructions, in a 7300 Real Time PCR system (Applied Biosystems; Thermo Fisher Scientific, Inc.). The thermocycling conditions were as follows: 95˚C for 20 sec, followed by 40 cycles of 15 sec at 95˚C and annealing/extension for 45 sec at 60˚C. The primers were synthesized and purchased from Bioneer Corp., and the sequences were as follows: SQSTM1 forward, 5'-ATCGGAG GATCCGAGTGT-3' and reverse, 5'-TGGCTGTGAGCTGCT CTT-3'; β-actin forward, 5'-CAACTGGGACGACATGGAG AAAAT-3' and reverse, 5'-CCAGAGGCGTACAGGGATAGC AC-3'. The relative mRNA expression levels of p62 were normalized to β-actin following the $2^{-\Delta\Delta Cq}$ method (21).

ELISA analysis. Interleukin-18 (IL-18) levels from culture media was measured with an ELISA kit from R&D Systems,

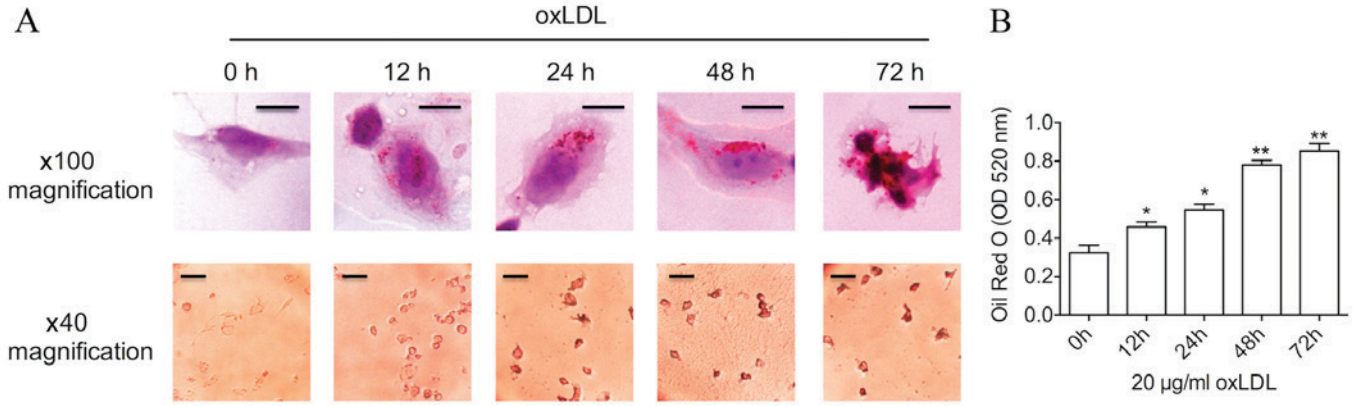

Figure 1. Prolonged oxLDL stimulation results in advanced foam cell formation. (A) THP-1-derived macrophages were incubated with 20 μg/ml oxLDL for 0, 12, 24, 48 and 72 h. Additionally, Oil Red O staining was used to label foam cells, which was imaged by a bright-filed microscope. Upper panels: Magnification, x100; scale bar, 10 μm. Lower panels: Magnification, x40; scale bar, 50 μm. (B) The graph represents OD values at 520 nm of ~1x10^6 cells/ml isopropanol. Data represent the mean ± standard deviation of six independent experiments. *P<0.05 and **P<0.01 vs. 0 h. oxLDL, oxidized low-density lipoprotein; OD, optical density.

Inc., (cat. no. 7620; Minneapolis, MN, USA), according to the manufacturer's instructions.

Evaluation of cell viability by MTT assay. An MTT cell viability/cytotoxicity kit was used that was purchased from Beyotime Institute of Biotechnology (Shanghai, China). In total, ~10,000 cells were plated in each well of 96-well plates. Following the treatment with oxLDL and siRNA, 20 μl MTT reagent (5 mg/ml) was added to each well and the cells were then cultured for 4 h at 37˚C. Subsequently, the supernatant was removed and 150 μl dimethyl sulfoxide (DMSO) was added to each well to dissolve formazan. A well with DMSO but without cells was used as a control, and the OD value of each well was detected at 490 nm using a Lumo microplate reader (PHOMO; Autobio Diagnostics Co., Ltd., Shanghai, China). Cell viability was expressed as a percentage of the untreated control.

Annexin V/propidium iodide (PI) double staining and fluorescence-activated cell sorting (FACS) analysis. Following the treatment with oxLDL and siRNA, THP-M cells maintained in 10% FBS-RPMI-1640 were collected, re-suspended and stained with Annexin V-fluorescein isothiocyanate/PI (Annexin V/PI apoptosis kit; BD Biosciences, Franklin Lakes, NJ, USA), according to the manufacturer's instructions. A total of 1x10^4 cells from each sample (con siRNA treated and p62 siRNA treated samples, respectively) were stained with 5 μl Annexin V and 5 μl propidium iodide (PI) for 15 min in the dark at room temperature, then re-suspended in 400 μl calcium binding solution, and analyzed on a FACSCanto II flow cytometer (BD Biosciences). Data analysis was performed with BD FACSDiva v8.0.1 software (BD Biosciences). The percentage of Annexin V-positive/PI-negative (considered as apoptotic cells) and Annexin V-positive/PI-positive (considered as necrotic cells) staining was determined and compared with the control groups.

Statistical analysis. All numerical data and error bars were provided as the mean ± standard deviation. Statistical significance of the differences among groups was analyzed using GraphPad Prism 6.0 software (GraphPad Software, Inc., La Jolla, CA, USA). Multi-group comparisons of the mean data were performed using one-way analysis of variance with the Student-Newman-Keuls test. P<0.05 was considered to indicate a statistically significant difference.

Results

Prolonged oxLDL treatment results in advanced foam cell formation. THP-1-derived foam cell models were established using oxLDL, one of the best-known atherogenic lipoproteins (10), in order to elevate intracellular cholesterol levels. Firstly, a time course of changes in lipid levels was examined during the process of foam cell formation. As demonstrated in Fig. 1, following treatment with a common dose (20 μg/ml) of oxLDL, Oil Red O staining and oxLDL uptake assay revealed a time-dependent increase in lipid levels within the THP-M cells. Furthermore, incubation with oxLDL for a 48-h period induced an increase in the size of lipid droplets in the cytoplasm, as assessed by bright-filed microscopy, which was a typical characteristic of foam cells. Several cells even burst when cultured with oxLDL for 72 h, suggesting that advanced foam cells had been formed. Oil Red O staining was significantly increased following 12, 24 (both P<0.05), 48 and 72 h (both P<0.01) of oxLDL treatment compared with 0 h.

Prolonged oxLDL treatment induces p62 protein accumulation during foam cell formation. Data of immunoblotting revealed a significantly reduced level of p62 protein after 24 h of oxLDL treatment compared with 0 h (P<0.01). However, during prolonged oxLDL treatment, at 48 and 72 h, the p62 level increased significantly compared with the level at 24 h (P<0.01), and the level at 72 h was more than the basal level (P<0.05; Fig. 2A and B). These data indicated that oxLDL is involved in the regulation of the p62 protein level, and prolonged oxLDL exposure leads to elevated expression of p62 in advanced foam cells. Following this, the transcription level of SQSTM1 mRNA in THP-M cells with oxLDL treatment was assessed. It was demonstrated that during the first 48 h of oxLDL treatment, SQSTM1 mRNA was significantly

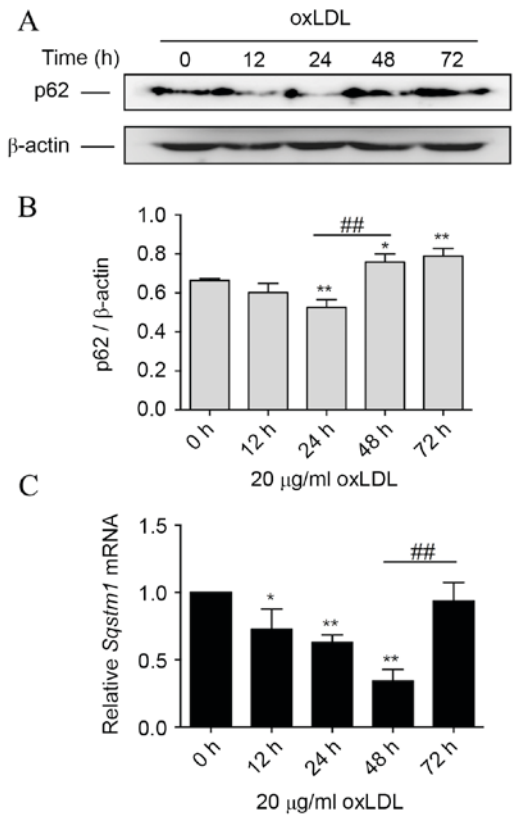

Figure 2. oxLDL influences the expression of p62 at the protein and mRNA levels. (A) Time course of p62 protein expression in THP-M cells treated with oxLDL (20 μg/ml). Western blotting experiments were performed on total protein extracts using anti-p62 antibody, and β-actin expression was used as a loading control. (B) The graph represents values of p62 band intensity following normalization to β-actin by densitometry. (C) Reverse transcription-quantitative polymerase chain reaction experiments of SQSTM1 mRNA expression in THP-M cells treated with 20 μg/ml oxLDL for 0, 12, 24, 48 and 72 h. Relative SQSTM1 mRNA levels were normalized to β-actin mRNA. Data represent the mean ± standard deviation of three independent experiments *P<0.05 and **P<0.01 vs. 0 h; $^{\#\#}$P<0.01 as indicated. oxLDL, oxidized low-density lipoprotein; THP-M, THP-1-derived macrophages; SQSTM1, sequestosome-1.

decreased compared with that at 0 h (P<0.05). Notably, the SQSTM1 mRNA level then significantly increased following oxLDL treatment for 72 h (P<0.01), compared with the level at 48 h, to almost the basal level at 0 h (Fig. 2C).

Knockdown of p62 leads to a decrease in IL-18 secretion from macrophages with prolonged oxLDL exposure. Given the multiple pathophysiological roles of p62 reported in studies on other diseases, the present study aimed to determine the potential role of p62 accumulation in advanced foam cells. IL-18, one of the pro-inflammatory cytokines in atherosclerosis, is produced from NLR family pyrin domain containing 3 inflammasome activation and may be regulated through the NF-κB pathway (22). In order to examine whether increased p62 protein levels were associated with oxLDL-induced IL-18 secretion, THP-M cells were treated with siRNA against p62. Compared with the con siRNA group, and after oxLDL treatment for the indicated time, p62 siRNA led to a significant decrease in the expression of p62 protein by 41.3% at 24 h and 62.0% at 72 h (P<0.05; Fig. 3A). On the transcriptional level, the p62 siRNA treatment group revealed a significant reduction of SQSTM1 mRNA to 47.8% at 24 h and 30.2% at 72 h (P<0.05; Fig. 3B).

Time course experiments demonstrated that oxLDL gradually induced IL-18 secretion from macrophages, and prolonged oxLDL treatment markedly raised IL-18 levels. Although no significant difference was observed for the first 24 h between the con and p62 siRNA groups, 48-h and 72-h oxLDL-treated cells revealed a significant reduction in IL-18 secretion in the presence of p62 siRNA compared with those treated with con siRNA (P<0.01; Fig. 3C). These results indicated that cytoplasmic accumulation of p62 mediates oxLDL-induced IL-18 secretion in THP-M cells, which implies that p62 could serve as a proinflammatory stimulus in advanced foam cells.

Knockdown of p62 exhibits positive effects against prolonged oxLDL-induced cell death. Although cell death has been extensively described in numerous oxLDL studies (5,7,10), the underlying mechanism remains unclear. As previous reports have demonstrated, ubiquitinated protein caspase-8 could interact with p62 and initiate a non-death receptor-mediated pathway of apoptotic cell death (23). Therefore, the increased p62 level in advanced foam cells could be detrimental to cell survival. In order to examine whether p62 was functionally involved in oxLDL-induced macrophage death, knockdown approaches were used in THP-M cells, and the changes of cell viability were evaluated for the indicated time.

As depicted in Fig. 3D, for the first 24 h of oxLDL treatment, there was no significant difference between con and p62 siRNA-treated cells. However, following prolonged incubation with oxLDL, the viability of con siRNA-treated THP-M cells was reduced, and p62 siRNA-treated cells revealed a significant increase in cell viability at 48 and 72 h after oxLDL treatment compared with con siRNA-treated cells (P<0.05). Subsequently, the apoptotic and necrotic rates of THP-M cells were measured by flow cytometry following treatment with oxLDL for 72 h. Data demonstrated that silencing p62 significantly attenuated prolonged oxLDL-induced cell necrosis compared with the con siRNA cells (P<0.01; Fig. 3E). This suggested a novel cytotoxic role of p62 in foam cell progression.

Knockdown of p62 improves autophagic activity and dampens foam cell formation. Autophagic activity, including both autophagic initiation and flux, involves the fusion of cargo-laden autophagosomes with lysosomes and results in cargo degradation within the lysosome (24). The LC3 conjugation system is critical to autophagy. Cytosolic LC3 (LC3-I) is processed and converted to the phosphatidylethanolamine-conjugated form (LC3-II), which is located on the autophagosomal membrane and thus commonly used as an autophagosomal indicator (25). Notably, compared with con siRNA-treated cells, p62 siRNA-treated cells revealed a significant switch of LC3-I to LC3-II (P<0.01; Fig. 4A and B), indicating that autophagic initiation was activated by p62 inhibition. Following this, the activity of autophagic flux was assessed using CQ. LC3-II in p62 siRNA-treated cells was further increased in the presence of CQ at 0 and 72 h compared with cells treated with only p62 siRNA (P<0.05), which represented the completed autophagic process (Fig. 4A and C). A previous study revealed that autophagy regulates cholesterol efflux from

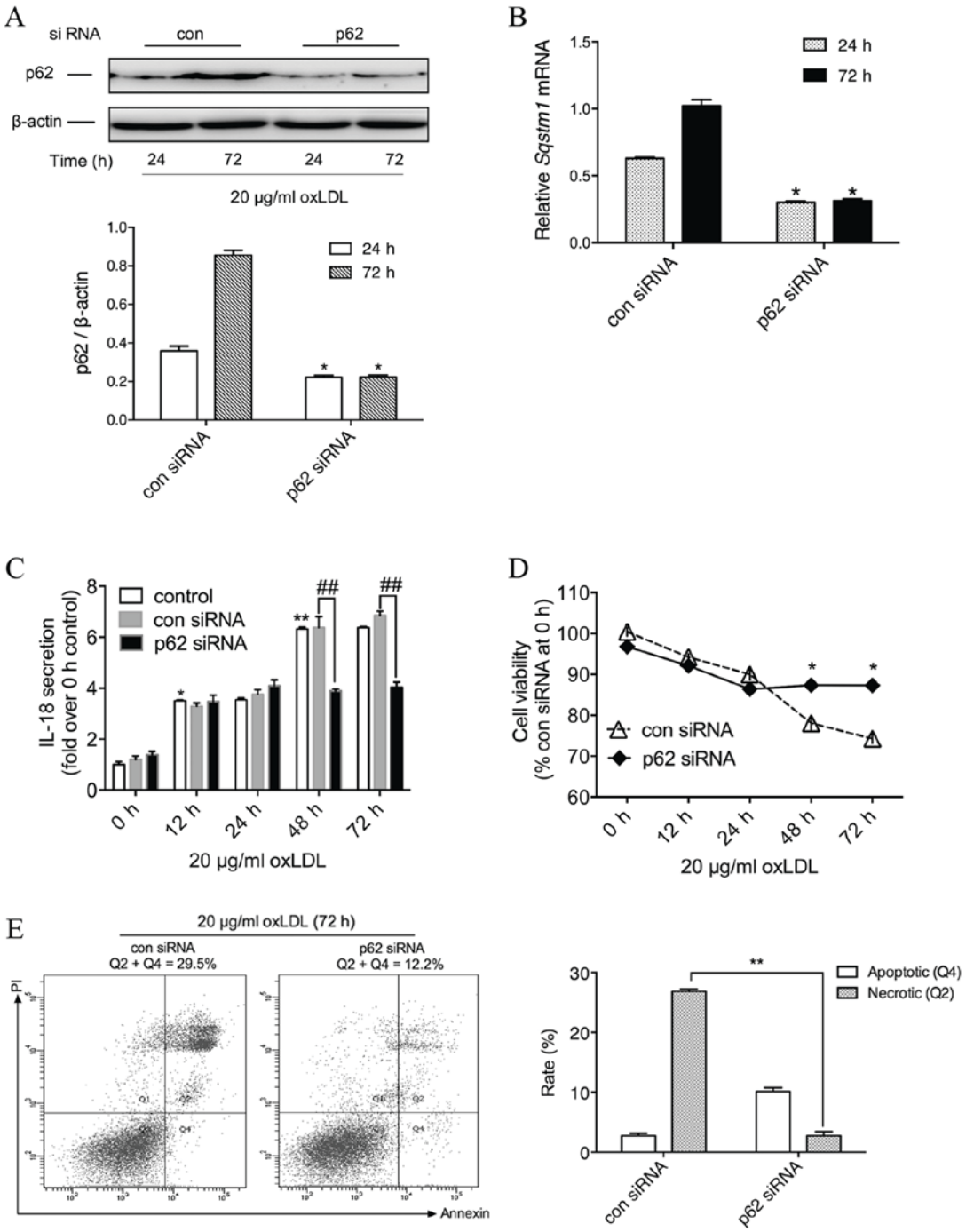

Figure 3. Silencing p62 reduces IL-18 secretion and promotes cell survival of macrophages with prolonged oxLDL exposure. (A) THP-M cells treated with oxLDL (20 μg/ml) for the indicated time following transfection with 50 nM con siRNA or p62 siRNA. Western blotting experiments were performed on total protein extracts using anti-p62 antibody, and β-actin expression was used as a loading control. The graph represents the values of p62 band intensity after normalization to β-actin by densitometry. *P<0.05 vs. 24 h group. (B) The graph represents values of the SQSTM1 mRNA expression following normalization for β-actin mRNA by reverse transcription-quantitative polymerase chain reaction. *P<0.05 vs. 24 h group. (C) ELISA of secreted IL-18 in the media of cells treated with con or p62 siRNA and 20 μg/ml oxLDL for 0, 12, 24, 48 and 72 h. *P<0.05 and **P<0.01 vs. 0 h; $^{\#\#}$P<0.01 as indicated. (D) THP-M cells were pretreated with con or p62 siRNA and then treated with 20 μg/ml oxLDL for the indicated times. Cell viability was analyzed by the MTT assay. Results are expressed as a percentage of con siRNA group at 0 h. *P<0.05 vs. con siRNA group. (E) Determination of cell death by flow cytometry of Annexin V-fluorescein isothiocyanate/PI staining in THP-M cells transfected with con or p62 siRNA and then incubated with oxLDL (20 μg/ml) for the indicated times. Data are representatives of three independent experiments. **P<0.01 as indicated. IL, interleukin; oxLDL, oxidized low-density lipoprotein; THP-M, THP-1-derived macrophages; siRNA, small interfering RNA; con, control; PI, propidium iodide.

macrophage foam cells (26). Therefore, it was hypothesized that silencing p62 could prevent oxLDL-induced lipid deposition in macrophages. Results from Oil Red O staining revealed that THP-M cells exposed to 72 h of oxLDL exhibited a significantly reduced number and size of lipid droplets in the presence of p62 siRNA compared with those treated with oxLDL and con siRNA (P<0.05; Fig. 4D), indicating that reducing the p62 level could effectively dampen foam cell formation.

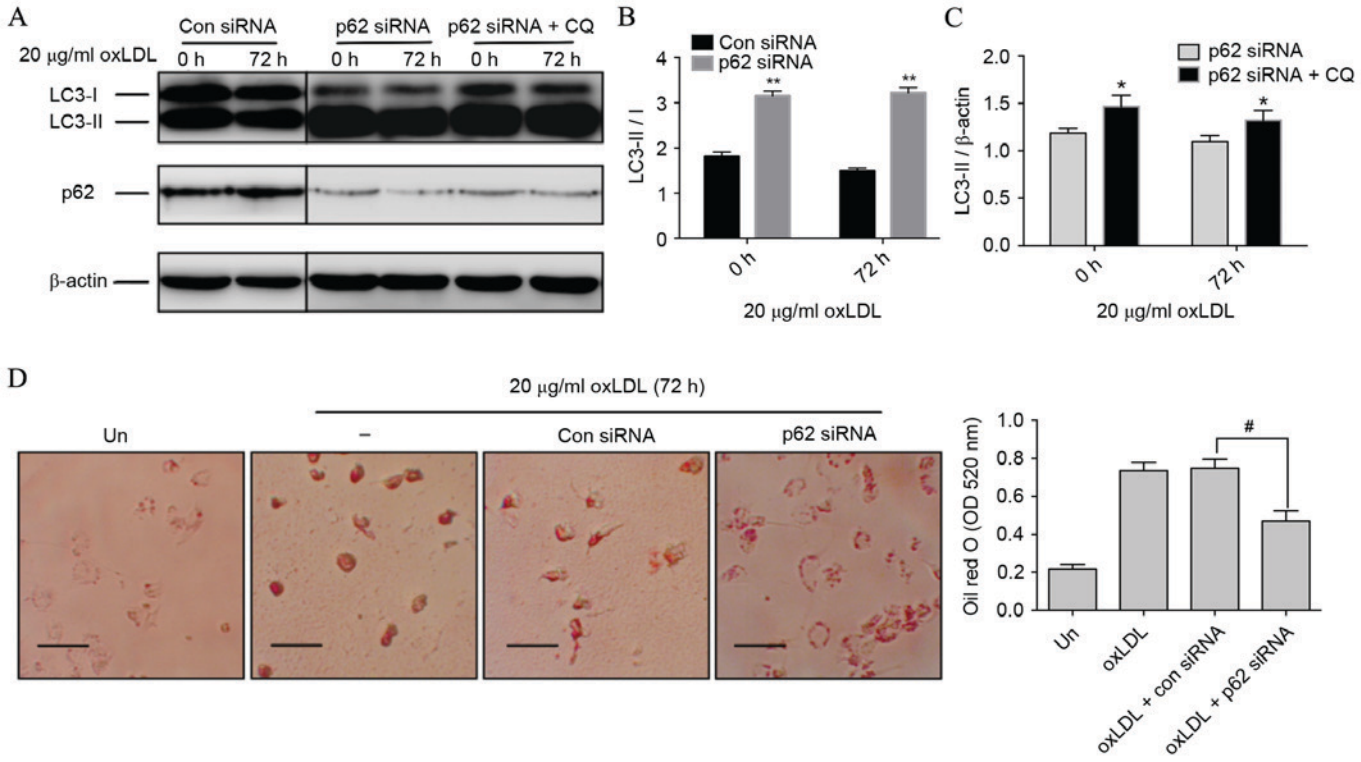

Figure 4. Silencing p62 improves autophagic activity and dampens foam cell formation. (A) THP-M cells were transfected with con or p62 siRNA. Western blot analysis was performed with the anti-LC3B antibody following exposure to 20 μg/ml oxLDL for the indicated time, with or without CQ (30 μM) for the last 2 h. β-actin expression was used as a protein loading control. (B) Densitometric quantification of LC3-II/I from the western blot analysis of cells treated with con or p62 siRNA. (C) Densitometric quantifications of LC3-II from the western blot analysis of cells treated with p62 siRNA with or without CQ. (D) THP-M cells were treated with con or p62 siRNA for 48 h before stimulation with 20 μg/ml oxLDL for 72 h. Foam cells were then assayed by Oil red O staining and imaged by a bright-filed microscope (magnification, x40). Scale bar, 50 μm. The graph represents OD values at 520 nm of ~1x10^6 cells/ml isopropanol. Data represent the mean ± standard deviation of three independent experiments. **P<0.01 vs. con siRNA; *P<0.05 vs. p62 siRNA; $^{\#}$P<0.05 as indicated. THP-M, THP-1-derived macrophages; siRNA, small interfering RNA; con, control; '-', oxLDL treated cells without any siRNA; Un, untreated cells; LC3, light-chain 3; oxLDL, oxidized low-density lipoprotein; CQ, chloroquine; OD, optical density.

Discussion

As a cytosolic protein, the expression of p62 may be regulated in two ways: Generation and degradation. It was worth noting that, although treatment with oxLDL for a 48-h period caused an increase in p62 protein, the transcriptional level of SQSTM1 was significantly downregulated in the present study. This difference suggested that degradation pathway autophagic dysfunction may be involved in the regulation of p62 expression within oxLDL-treated macrophages.

A previous study has indicated that either excessive lipid concentrations or chronic lipid exposure possesses the property of inhibiting autophagy by blocking the fusion of autophagic/lysosomal compartments or impairing lysosomal acidification and hydrolase activity (27), which was mostly consistent with the observations of the present study. By silencing the expression of p62 in the present study, decreased IL-18 secretion and reduced overall cell death was observed in prolonged oxLDL-treated cells. Accordingly, these results indicated a proinflammatory and cytotoxic role of p62 in foam cell progression. Notably, silencing p62 significantly decreased the necrosis rate in prolonged oxLDL-treated macrophages. However, the specific mechanism of this remains to be discussed in the future.

One surprising observation of the present study was that, in the RNA interference experiments, p62 siRNA-treated THP-M cells revealed an evident increase in LC3 conversion, and the autophagic flux remained normal even after a 72-h incubation with oxLDL. These results indicated that p62 may negatively regulate autophagic activity, and these findings are further supported by a previous study that demonstrated that p62-silencing induced LC3-II expression and autophagy activation by inhibiting mTOR in numerous p62-overexpressed carcinoma cells (28).

Furthermore, results from a previous study reported that mTOR-silencing markedly suppressed foam cell formation with a decrease in lipid deposition by upregulating autophagy (29). This report extends our thought and may help explain another observation of the present study, which demonstrated an evident decrease in lipid accumulation in prolonged oxLDL-treated THP-M cells in the presence of p62 siRNA. It has been reported that the autophagic substrate p62 promotes mTOR complex 1 (mTORC1) activity by interacting with its key component, Raptor (30,31). mTORC1 also has a negative role in the regulation of autophagy, which contributes to cholesterol efflux (25). Therefore it is hypothesized that silencing p62 activates mTORC1, thus enhancing autophagic activity and leading to augmented reverse cholesterol transport and restrained foam cell formation. In addition, the discovery of silencing p62 inducing autophagy activation provides a way to understand how p62 influences efferocytosis. A previous study reported that apoptotic cells that die with defective

autophagy are poorly engulfed by efferocytes (32). Therefore, it is presumed that silencing p62 boosts autophagy, which is beneficial to effective efferocytosis against secondary necrosis.

In light of the above points, the present study demonstrated an important role for p62 in the nexus of autophagy activation, lipid metabolism, inflammatory response and cell death during foam cell progression. Such an interrelationship may trap macrophages into a detrimental reinforcing loop, in which prolonged oxLDL exposure promotes p62 accumulation, as well as lipid deposition. Next, accumulated p62 further inhibits autophagy, which in turn leads to more p62 accumulation and accelerates foam cell formation, with growing inflammation and cell death.

The observations of the present study highlight a previously unexplored interrelationship between p62 regulation and lipid metabolism in macrophages, and provide novel insight into how the plaque switches to an unstable state, allowing us to further understand the significance of accumulated p62 in atherosclerotic plaques. Besides being a marker of defective autophagy in macrophages, p62 may also be a detrimental factor that triggers increased inflammation and cell death. In addition, knowledge gained from the present study of p62 in foam cells may be useful for devising mechanism-based therapeutic strategies. Therefore, more cell lines, lipid types and even *in vivo* studies are required in the future to establish the actual relationship between the regulation of p62 in macrophage foam cells and atherosclerosis.

Acknowledgements

The present study was supported by the China Postdoctoral Science Foundation funded project of Heilongjiang Province (grant no. LBH-Q12033).

References

1. World Health Organization (WHO): A global brief on hypertension: Silent killer, global public health crisis (World Health Day 2013). http://apps.who.int/iris/bitstream/10665/79059/1/WHO_DCO_WHD_2013.2_eng.pdf. Accessed Feb 11, 2015.
2. Libby P, Ridker PM and Hansson GK: Progress and challenges in translating the biology of atherosclerosis. Nature 473: 317-325, 2011.
3. Finn AV, Nakano M, Narula J, Kolodgie FD and Virmani R: Concept of vulnerable/unstable plaque. Arterioscler Thromb Vasc Biol 30: 1282-1292, 2010.
4. Glass CK and Witztum JL: Atherosclerosis: The road ahead. Cell 104: 503-516, 2001.
5. Mestas J and Ley K: Monocyte-endothelial cell interactions in the development of atherosclerosis. Trends Cardiovasc Med 18: 228-232, 2008.
6. Kleemann R, Zadelaar S and Kooistra T: Cytokines and atherosclerosis: A comprehensive review of studies in mice. Cardiovasc Res 79: 360-376, 2008.
7. Stewart CR, Stuart LM, Wilkinson K, van Gils JM, Deng J, Halle A, Rayner KJ, Boyer L, Zhong R, Frazier WA, *et al*: CD36 ligands promote sterile inflammation through assembly of a Toll-like receptor 4 and 6 heterodimer. Nat Immunol 11: 155-161, 2010.
8. Liao X, Sluimer JC, Wang Y, Subramanian M, Brown K, Pattison JS, Robbins J, Martinez J and Tabas I: Macrophage autophagy plays a protective role in advanced atherosclerosis. Cell Metab 15: 543-553, 2012.
9. Razani B, Feng C, Coleman T, Emanuel R, Wen H, Hwang S, Ting JP, Virgin HW, Kastan MB and Semenkovich CF: Autophagy links inflammasomes to atherosclerotic progression. Cell Metab 15: 534-544, 2012.
10. Moore KJ and Tabas I: Macrophages in the pathogenesis of atherosclerosis. Cell 145: 341-355, 2011.
11. Sergin I and Razani B: Self-eating in the plaque: What macrophage autophagy reveals about atherosclerosis. Trends Endocrinol Metab 25: 225-234, 2014.
12. Maiuri MC, Grassia G, Platt AM, Carnuccio R, Ialenti A and Maffia P: Macrophage autophagy in atherosclerosis. Mediators Inflamm 2013: 584715, 2013.
13. Komatsu M and Ichimura Y: Physiological significance of selective degradation of p62 by autophagy. FEBS Lett 584: 1374-1378, 2010.
14. Manley S, Williams JA and Ding WX: Role of p62/SQSTM1 in liver physiology and pathogenesis. Exp Biol Med (Maywood) 238: 525-538, 2013.
15. Bitto A, Lerner CA, Nacarelli T, Crowe E, Torres C and Sell C: P62/SQSTM1 at the interface of aging, autophagy and disease. Age (Dordr) 36: 9626, 2014.
16. Lee HM, Shin DM, Yuk JM, Shi G, Choi DK, Lee SH, Huang SM, Kim JM, Kim CD, Lee JH and Jo EK: Autophagy negatively regulates keratinocyte inflammatory responses via scaffolding protein p62/SQSTM1. J Immunol 186: 1248-1258, 2011.
17. Burdelski C, Reiswich V, Hube-Magg C, Kluth M, Minner S, Koop C, Graefen M, Heinzer H, Tsourlakis MC and Wittmer C: Cytoplasmic accumulation of sequestosome 1 (p62) is a predictor of biochemical recurrence, rapid tumor cell proliferation, and genomic instability in prostate Cancer. Clin Cancer Res 21: 3471-3479, 2015.
18. Schrijvers DM, De Meyer GR, Kockx MM, Herman AG and Martinet W: Phagocytosis of apoptotic cells by macrophages is impaired in atherosclerosis. Arterioscler Thromb Vasc Biol 25: 1256-1261, 2005.
19. Murase Y, Kobayashi J, Nohara A, Asano A, Yamaaki N, Suzuki K, Sato H and Mabuchi H: Raloxifene promotes adipocyte differentiation of 3T3-L1 cells. Eur J Phamacol 538: 1-4, 2006.
20. Choi SH, Gonen A, Diehl CJ, Kim J, Almazan F, Witztum JL and Miller YI: SYK regulates macrophage MHC-II expression via activation of autophagy in response to oxidized LDL. Autophagy 11: 785-795, 2015.
21. Livak KJ and Schmittgen TD: Analysis of relative gene expression data using real-time quantitative PCR and the 2(-Delta Delta C(T)) method. Methods 25: 402-408, 2001.
22. Badimon L: Interleukin-18: A potent pro-inflammatory cytokine in atherosclerosis. Cardiovasc Res 96: 172-175, 2012.
23. Zhang YB, Gong JL, Xing TY, Zheng SP and Ding W: Autophagy protein p62/SQSTM1 is involved in HAMLET-induced cell death by modulating apoptosis in U87MG cells. Cell Death Dis 4: e550, 2013.
24. Kim KH and Lee MS: Autophagy-a key player in cellular and body metabolism. Nat Rev Endocrinol 10: 322-337, 2014.
25. Kabeya Y, Mizushima N, Ueno T, Yamamoto A, Kirisako T, Noda T, Kominami E, Ohsumi Y and Yoshimori T: LC3, a mammalian homologue of yeast Apg8p, is localized in autophagosome membranes after processing. EMBO J 19: 5720-5728, 2000.
26. Ouimet M, Franklin V, Mak E, Liao X, Tabas I and Marcel YL: Autophagy regulates cholesterol efflux from macrophage foam cells via lysosomal acid lipase. Cell Metab 13: 655-667, 2011.
27. Koga H, Kaushik S and Cuervo AM: Altered lipid content inhibits autophagic vesicular fusion. FASEB J 24: 3052-3065, 2010.
28. Nihira K, Miki Y, Ono K, Suzuki T and Sasano H: An inhibition of p62/SQSTM1 caused autophagic cell death of several human carcinoma cells. Cancer Sci 105: 568-575, 2014.
29. Wang X, Li L, Niu X, Dang X, Li P, Qu L, Bi X, Gao Y, Hu Y and Li M: mTOR enhances foam cell formation by suppressing the autophagy pathway. DNA Cell Biol 33: 198-204, 2014.
30. Ichimura Y, Kumanomidou T, Sou YS, Mizushima T, Ezaki J, Ueno T, Kominami E, Yamane T, Tanaka K and Komatsu M: Structural basis for sorting mechanism of p62 in selective autophagy. J Biol Chem 283: 22847-22857, 2008.
31. Moscat J and Diaz-Meco MT: p62 at the crossroads of autophagy, apoptosis and cancer. Cell 137: 1001-1004, 2009.
32. Qu X, Zou Z, Sun Q, Luby-Phelps K, Cheng P, Hogan RN, Gilpin C and Levine B: Autophagy gene-dependent clearance of apoptotic cells during embryonic development. Cell 128: 931-946, 2007.